Sleep spindles are locally modulated by training on a brain–computer interface

Lise A. Johnson[a,b,1], Tim Blakely[c], Dora Hermes[d], Shahin Hakimian[e,f], Nick F. Ramsey[d], and Jeffrey G. Ojemann[a,g]

[a]University of Washington, Department of Neurological Surgery, Seattle, WA 98195; [b]The Center for Sensorimotor Neural Engineering, Seattle, WA 98105; [c]University of Washington, Department of Bioengineering, Seattle, WA, 98105; [d]Rudolf Magnus Institute of Neuroscience, University Medical Center Utrecht, Department of Neurology and Neurosurgery, Heidelberglaan 100, G03.124, 3584 CX, Utrecht, The Netherlands; [e]University of Washington Department of Neurology and [f]Regional Epilepsy Center at Harborview Medical Center, Seattle, WA 98104; and [g]Seattle Children's Research Institute, Seattle, WA 98145

Edited by Marcus E. Raichle, Washington University in St. Louis, St. Louis, MO, and approved September 27, 2012 (received for review May 7, 2012)

The learning of a motor task is known to be improved by sleep, and sleep spindles are thought to facilitate this learning by enabling synaptic plasticity. In this study subjects implanted with electrocorticography (ECoG) arrays for long-term epilepsy monitoring were trained to control a cursor on a computer screen by modulating either the high-gamma or mu/beta power at a single electrode located over the motor or premotor area. In all trained subjects, spindle density in posttraining sleep was increased with respect to pretraining sleep in a remarkably spatially specific manner. The pattern of increased spindle activity reflects the functionally specific regions that were involved in learning of a highly novel and salient task during wakefulness, supporting the idea that sleep spindles are involved in learning to use a motor-based brain–computer interface device.

The need for sleep is ubiquitous in the animal kingdom, but the purpose of sleep is still poorly understood and controversial in many respects. Nevertheless, it is now widely accepted that sleep, and especially nonrapid eye movement (NREM) sleep, plays an active role in learning and memory consolidation (1). NREM epochs are easily identified in the cortical field potential as periods dominated by high-amplitude, low-frequency oscillations (2). Sleep spindles are one of the most prominent and recognizable of these oscillations, and as such they are commonly used to classify NREM sleep stages. These brief 12- to 15-Hz oscillations are generated by the reticular nucleus of the thalamus and grouped by the slow oscillation (<1 Hz) in the neocortex (3). The reticular nucleus is involved in gating sensory inputs and it is hypothesized that sleep spindles prevent incoming sensory information from reaching the neocortex during NREM sleep (4). This dissociation could provide a window for uninterrupted replay of recently instantiated memories and thus support sleep-dependent memory consolidation. There is now a large body of evidence linking sleep spindles to learning and memory in both humans and animals (5–7). For example, increases in spindle density have been correlated with learning a declarative memory task (5), with retention of verbal memories (6), and with relevant recall of a remote memory (7). Additionally, spindles are correlated with sharp-wave complexes in the hippocampus (8, 9) and are associated with stored-trace reactivation in the neocortex (10). It has been hypothesized that sleep spindles actually facilitate learning by establishing a cortical state that is conducive to synaptic plasticity, and therefore, to sleep-dependent memory consolidation (11, 12). A great deal of emphasis has been placed on the role of sleep spindles in the hippocampal–neocortical dialogue (8, 9, 13), and thus consolidation of hippocampal-dependent memories. However, there is ample data to suggest that spindles are also important for motor and procedural learning (14–17).

This theory is complicated by the fact that, whereas learning requires changes to specific circuits, spindles have traditionally been considered global events arising from a single generator. However, several studies have shown that this assumption requires reevaluation. Nishida and Walker (17) showed that following procedural task learning, spindles were increased in the learning hemisphere with respect to the nonlearning hemisphere. More recently there has been a report that spindles recorded by magnetoencephalography, in contrast to those recorded by EEG, arise from multiple asynchronous generators (18), a result which may be explained by the interaction of core and matrix thalmocortical projections (19). The globally synchronous nature of spindles was further challenged by Nir et al. (20) who used depth electrodes implanted in medial brain areas to show that the majority of sleep spindles are not synchronous across the brain but rather localized to a single brain area. However, the extent of the locality of spindles within a brain area has not yet been demonstrated. Furthermore, it has not been shown that local groups of spindles are independently modulated by behavior.

In this study, subjects implanted with subdural electrode grids for epilepsy monitoring were trained to control a computer cursor by modulating the activity at a single electrode. Here we show that after training on a brain–computer interface (BCI) the rate of sleep spindle occurrence in posttraining sleep is increased in a remarkably localized pattern around the functionally specific regions that were involved in task performance.

Results

Of the five subjects that participated in this study, three were trained on the task and two served as controls. In all subjects, functional screening confirmed that the implanted grid provided coverage of primary motor and/or premotor areas; in all subjects the epileptic focus was determined to be outside of these areas. The three test subjects were trained to control a computer cursor in one dimension, first with overt movement and later with motor imagery. Cursor position was modulated by the power in either the high-gamma or mu/beta band measured at a single electrode (the task electrode) over primary motor or premotor cortex. Mu/beta (10–30 Hz) is a motor rhythm that broadly decreases in power over motor areas in response to movement or imagined movement (21). In contrast, power in the high-gamma (70–100 Hz) band increases very locally in response to specific motor movement or imagery (22). Both signals have been successfully used for BCI control (23–25). During each task trial, a cursor was presented vertically centered on the far left side of the screen and moved at a fixed rate across the screen to the right side. The vertical velocity of the cursor was updated every 40 ms based on the power in the specified frequency band recorded at the task electrode. The subject was asked to control the cursor such that when it reached the far right side of the screen its vertical position was within a designated target range. All subjects were given essentially the same instructions, but subjects were free to adopt whatever

Author contributions: L.A.J., N.F.R., and J.G.O. designed research; L.A.J., T.B., and D.H. performed research; S.H. contributed new reagents/analytic tools; L.A.J. analyzed data; and L.A.J. and J.G.O. wrote the paper.

The authors declare no conflict of interest.

This article is a PNAS Direct Submission.

[1]To whom correspondence should be addressed. E-mail: liseaj@uw.edu.

This article contains supporting information online at www.pnas.org/lookup/suppl/doi:10.1073/pnas.1207532109/-/DCSupplemental.

strategy they liked. For example, some subjects maintain a constant level of exertion throughout the duration of the trial, whereas others exert little effort for most of the trial and then ramp up activity at the end to hit the target. Empirically, a mu/beta-based BCI is more difficult to control than a high-gamma–based BCI.

The BCI task that was presented was highly novel, challenging, and salient for the subjects. Because subjects used real and/or imagined movement to control the cursor, it can be considered a *visuomotor* learning task, although lacking the tactile and proprioceptive sensory afferents that accompany normal movement. However, the learning of the procedural elements of the task cannot be separated from the memory of the experience of the task; the unprecedented nature of the task suggests a strong declarative memory component as well.

An automatic spindle detection algorithm was used to count the number of sleep spindles per minute recorded on every electrode during all identified NREM sleep epochs. The spindle rate during NREM on the day before training was compared with the spindle rate after training on the first training day.

In all of the trained subjects, the average spindle rate at the task electrode was significantly (rate ratio test, $P < 0.001$) increased following BCI training and a cluster pattern of spindle increases emerged around the task electrode (Fig. 1). Subjects 1 and 2 were trained on a high-gamma–based BCI. In subject 1, the task electrode was on the posterior edge of the precentral gyrus in Brodmann area 4 (primary motor cortex) (26). In subject 2, the task electrode was on the precentral gyrus at the boundary between Brodmann areas 4 and 6 (premotor cortex) (26). Subject 1 used real and imagined tongue movement to achieve control; subject 2 used real and imagined hand movement. In these two subjects the task electrode and one or two of its nearest neighbors (1-cm interelectrode distance) showed significant increases in spindle rate. Interestingly, in both of these subjects a broad pattern of decreased spindle rate appeared across the rest of the grid after training. Subject 3 was trained on a mu/beta-based BCI with an electrode on the posterior aspect of the middle frontal gyrus over Brodmann area 6 (premotor cortex) (26). This subject used real and imagined hand movement to control the cursor. The same clustering pattern appeared, but the effect was extended to second and third neighbors with tapering amplitude. This is partly accounted for by the fact the task electrode was on a minigrid, and thus its nearest neighbors were twice as close (0.5-cm interelectrode distance). The broader distribution of spindle increases may also have to do with the use of mu/beta as the control signal. Changes in the low-frequency motor rhythms have a greater spatial extent than changes in high gamma (27), which is thought to reflect an increase in local neural activity (22).

In control subjects who were not trained on the BCI task, some electrodes did show increases in spindle rate. This is not surprising, as these subjects participated in other activities during the day. However, the focally distributed pattern of rate increases observed after BCI training did not emerge in these subjects (Fig. 2).

The observation of localized spindle-rate modulation prompts several additional questions. For example, how localized are spindles? Do they occur on each electrode independently or on groups of electrodes at the same time? Does this change as a function of training? Are functionally related but physically separated areas modulated independently or together? To answer these questions, a method was developed to examine spindle comodulation across a population of electrodes. A coincidence measure was used to determine the extent of spindle comodulation between different electrodes; the coincidence was defined as the likelihood that a spindle would be detected on the first electrode within half a second of a spindle being detected on the second electrode. Comparison of pre- and posttraining sleep shows that electrodes have largely the same pattern of coincidence over both nights, and that this pattern is largely (but not uniformly) dominated by physical locality (Fig. 3 and see Fig. S6). A "distance" based on coincidence was used to hierarchically cluster electrodes into groups. Here these groups are referred to as networks but it should be understood that these networks are descriptive and have somewhat fluid boundaries based on the threshold that is chosen for clustering. The key point is that electrodes next to each other on the hierarchical clustering tree are more likely to have concurrent spindles regardless of where group boundaries are drawn. See Figs. S1–S5 for a more detailed view of these trees. Electrodes showing increases in spindle rate after training were invariably part of the same group (Fig. 4). In subject 1, two noncoincident and spatially distant groups showed increased rates. Only one of the groups was related to the BCI task; the other group was apparently modulated by an experimentally uncontrolled experience or an experimentally related process at a nontask electrode. In subject 2, only electrodes belonging to the same coincidence group as the task electrode

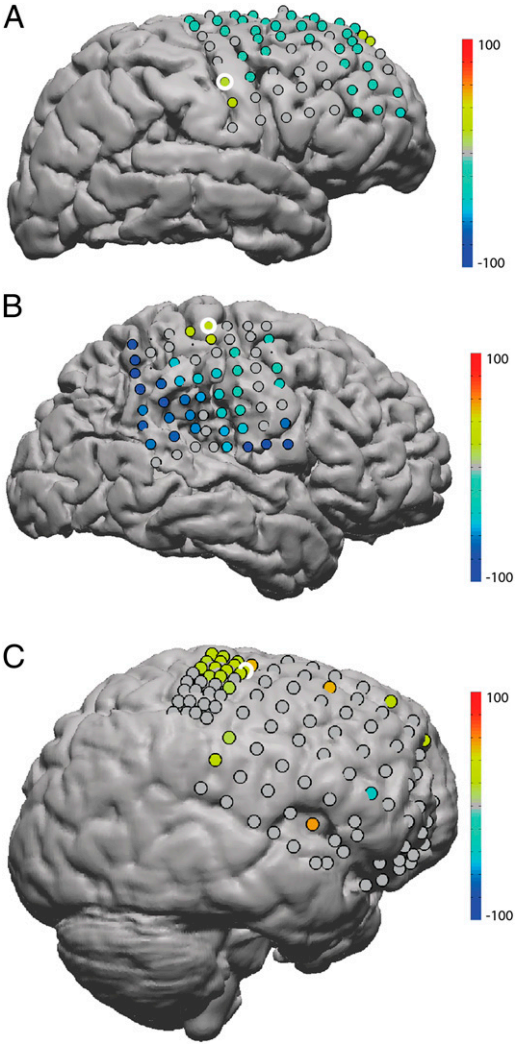

Fig. 1. Changes in spindle rate after training. For each electrode, the difference between the average rate of spindle occurrence in pre- and posttraining sleep is plotted on the subject's cortex as a percentage of the sum of the means. Warm colors indicate a rate increase; cool colors indicate a rate decrease. Electrodes that showed no significant ($P < 0.001$, Bonferroni corrected for multiple comparisons) change are drawn in gray. The electrode that was used for BCI control is circled in white. Subjects 1 (*A*) and 2 (*B*) were implanted with standard-sized grids (1 cm) and used high-gamma power for control. Subject 3 (*C*) was implanted with both a higher resolution (0.5 cm) and a standard-sized grid and used mu/beta power for control. Clusters of spindle-rate increases around the task electrode suggest that BCI training is responsible for the effect.

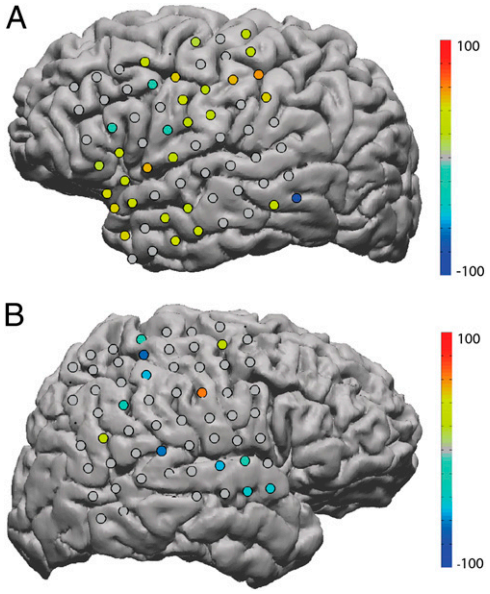

Fig. 2. Spindle-rate differences in control subjects. For each electrode, the difference between the average rate of spindle occurrence on two consecutive nights of sleep is plotted on the subject's cortex as a percentage of the sum of means. Warm colors indicate a rate increase; cool colors indicate a rate decrease. Electrodes that showed no significant ($P < 0.001$, Bonferroni corrected for multiple comparisons) change are drawn in gray. These subjects had coverage of motor areas but did not train on a BCI task. Both subjects 4 (*A*) and 5 (*B*) were implanted with standard-sized grids (1 cm). No focal clusters of spindle-rate increases are apparent.

showed increased rates. In subject 3, the coincidence group that includes the task electrode over the premotor cortex also includes electrodes over the primary hand motor cortex, and many of these electrodes showed increases in spindle rate after training. These results suggest that spindles in preexisting networks are differentially modulated based on training.

Discussion

A large and growing body of literature supports the involvement of NREM sleep in learning and memory of all sorts (28). Increasingly, sleep spindles, one of the most prominent features of NREM, have been implicated in these plastic processes (5, 7, 8, 17, 29). It has been postulated that spindles facilitate synaptic plasticity in cortical cells via calcium-dependent mechanisms (11), and it has been shown that cortical stimulation at the spindle frequency increases synaptic plasticity (30). If spindles are truly the carriers of memory consolidation, then they must act specifically on local circuits. Recent reports that spindles can occur independently in different medial brain areas suggest that spindles may have more of a local component than previously thought (20). Even so, these data cannot speak to whether spindles are localized within brain areas or whether local groups of spindles are specifically modulated by behavior.

One of the unique aspects of the BCI training is that successful performance is by design one-to-one correlated with activity in a small, well-defined part of the cortex. This, combined with the novelty, difficulty, and salience inherent to the task, presents an opportunity to examine how learning in local circuits impacts posttraining sleep. Our results show that following training on a BCI task, there was a specific increase in the rate of sleep spindles detected on the electrode used to control the BCI. Furthermore, a distinctive pattern of spindle-rate increases was observed for all three trained subjects. This pattern, which consisted of a cluster around areas known to be critically involved in the task, strongly suggests that the training was responsible for the effect. These results demonstrate that sleep spindles are not only locally manifested, but they are also locally modulated based on behavior. The observed spatially specific increases in spindle rate, taken together with previously reported findings, strongly support the hypothesis that sleep spindles facilitate motor-based learning in local circuits.

The generalized nature of these results is demonstrated by consistency between different subjects, different kinds of motor imagery (tongue vs. hand), different brain areas (primary motor cortex vs. premotor cortex), and even different control signals (mu/beta vs. high gamma). Additionally, subjects were recorded at two different research centers using different recording systems and parameters.

This study takes advantage of the regular arrangement of electrodes on the electrocorticography (ECoG) grid to determine the spatial extent of spindle networks on the surface of the neocortex. The coincidence of detected spindles between electrodes reveals that different spindle networks exist within the boundaries of the grid. Not surprisingly, neighboring electrodes tended to be part of the same coincidence network. However, these networks do not have a consistent spatial extent and the number of networks varies between subjects. Furthermore, in one subject, two sets of motor-related electrodes on different grids, although physically separated, were part of the same spindle network. This suggests that the network boundaries are determined by functional connectivity and not spatial proximity. In all of the subjects, the electrodes showing training-related increases in spindle rate were part of the same coincidence network. The coincidence pattern was highly similar between the pretraining night and the posttraining night, and thus it appears that behavioral-related changes in spindle rate are the result of a change in the gain on preexisting spindle networks and do not reflect a change in the pattern of connectivity, at least on this time scale.

Cortical sleep spindles are correlated with hippocampal sharp waves (8, 9) and stored-trace reactivation (10), and are therefore frequently associated with declarative memory processes. Other studies have shown that spindles increase in response to other kinds of learning as well (5, 7, 8, 17, 29), and this is confirmed by our results, which focus on what is essentially a motor task. This suggests that sleep spindles are involved in general mechanisms of cortical plasticity and not specific to hippocampal stored-trace reactivation.

Although these results are compelling, several caveats and potential confounds must be noted. These data were collected from epileptic patients who were not only tapering off of their antiseizure medication, but also taking pain medication. Epilepsy and sleep have a known interaction, and medications may affect sleep patterns (31). In addition, all of the subjects slept poorly with multiple arousals. Because the experimental schedule is determined by each subject's clinical and personal needs, the time of day when subjects trained on the task was not controlled, nor was the time between task performance and sleep onset. Spindle rate is known to be affected by multiple factors including age, sex, menstrual cycle, and intelligence (32–34). For this reason absolute differences in spindle rate should not be compared between subjects; instead a relative difference is used to measure within-subject changes.

In conclusion, these results are consistent with a scenario in which sleep spindles are generated in the thalamus, but gated by small, functionally connected networks in the neocortex. The gain on these "gates" is determined by the drive for plasticity in these networks, which is related to waking behavior, in this case, training on a BCI task.

Materials and Methods

Subjects. All subjects were patients undergoing long-term ECoG monitoring in preparation for surgical treatment of intractable epilepsy. Data were collected

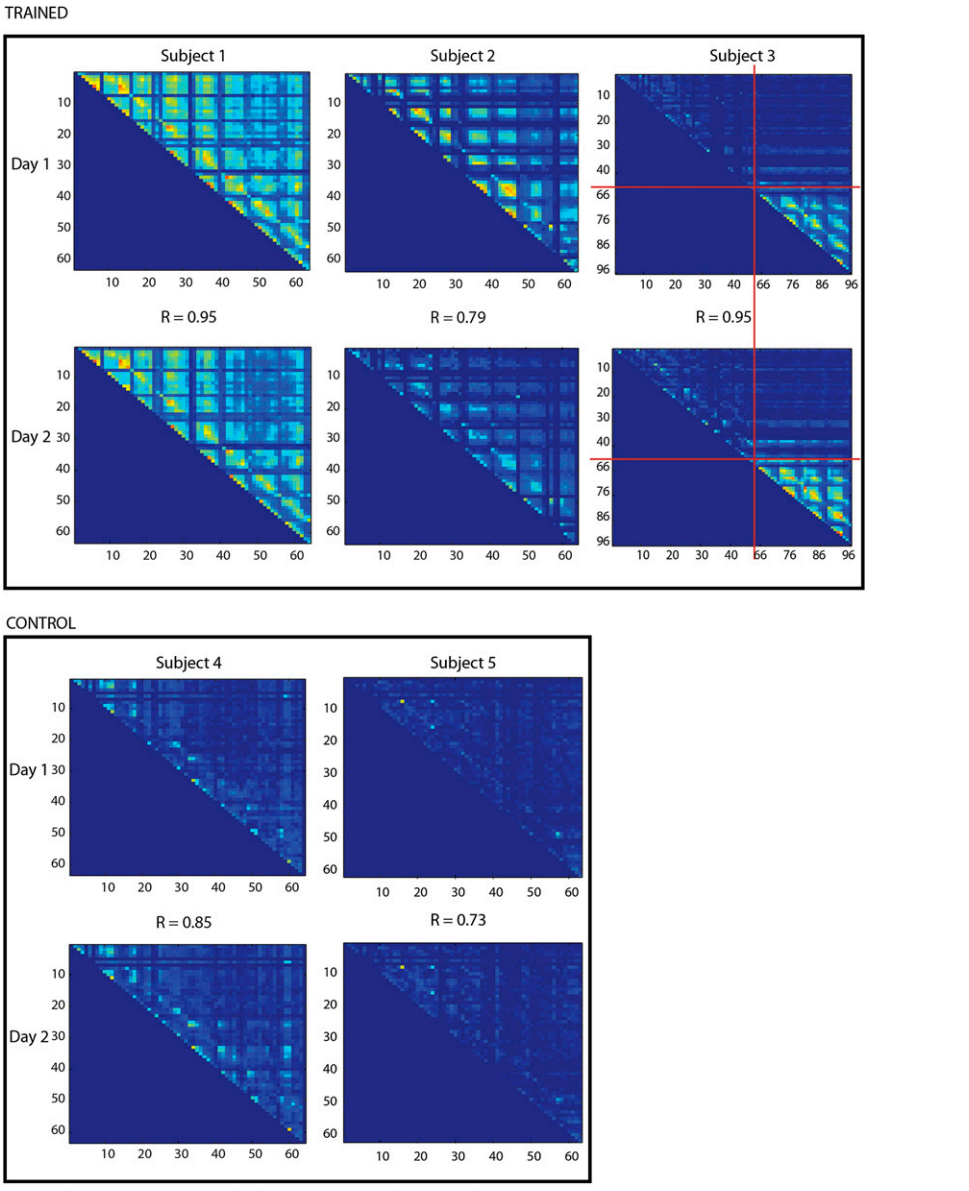

Fig. 3. Coincidence matrices. For each subject, the coincidence matrices for sleep on the first and second days are shown as heat maps. Complete coincidence is red; zero coincidence is blue. The pattern of coincidence is similar between the two nights as demonstrated by the correlation coefficient, *R*, which is shown between the two matrices. Electrodes are arranged from 1 to 64 for subjects 1, 2, 4, and 5 and from 1 to 48, and 65–96 for subject 3. Every increment of 8 represents the edge of the grid. In subject 3, electrodes 1–48 are on the regular grid and electrodes 65–96 are on the minigrid; the transition points between the two grids are marked by the red lines.

from five subjects (three female, ages 16–29) with subdural platinum electrode arrays (Ad-Tech) covering motor or premotor cortex. Decisions about electrode placement were based exclusively on clinical considerations. Electrodes on the standard-sized grids had a 2.3-mm exposed surface diameter and were spaced at 1 cm; electrodes on the minigrid were the same size, but the interelectrode distance was only 0.5 cm. Subjects 1, 2, 4, and 5 were patients at the University of Washington; subject 3 was a patient at Utrecht University Medical Center. All subjects gave informed consent according to the protocol approved by either the Seattle Children's Hospital and Regional Medical Center Institutional Review Board (University of Washington; subjects 1, 2, 4, and 5) or the Medical and Ethical Board of University Medical Center, Utrecht (subject 3). In three of the subjects, BCI experiments were performed 3–6 d after implantation of the electrode grid; sleep data were collected starting on the third day after surgery and continued for the duration of the monitoring (usually 7–10 d). Subjects 4 and 5 did not participate in the BCI experiments. Please see *SI Materials and Methods* for subject-specific methods and statistics as well as notes about potential confounds.

Recording. At the University of Washington, the ECoG signals were recorded by the XLTEK (Natus Medical) clinical monitoring system at a sampling rate of 500 (subjects 1 and 2), 1,000 (subject 2), or 2,000 Hz (subjects 4 and 5). The standard system parameters impose a high-pass filter at about 0.1 Hz. At Utrecht University Medical Center, the ECoG signals were recorded with a Mircromed system at 512 Hz and band-pass filtered between 0.15 and 134.4 Hz.

Data Preprocessing. Data were notch filtered to remove line noise at either 50 Hz (subject 3) or 60 Hz (all other subjects). Data sampled at rates greater than 500 Hz were antialias-filtered and downsampled to 500 Hz using the Matlab (MathWorks) "decimate" function.

Sleep Identification. Non-REM sleep epochs were identified by eye using the increased power in the delta band (1–6 Hz) and verified by the presence of K complexes and spindles. For every sleep epoch, all electrode traces were normalized by *z* scoring with respect to the amplitude in the 5- to 50-Hz range. This frequency range was chosen to eliminate the variable amplitude effects of K complexes, which have a maximum amplitude in medial–frontal regions (35).

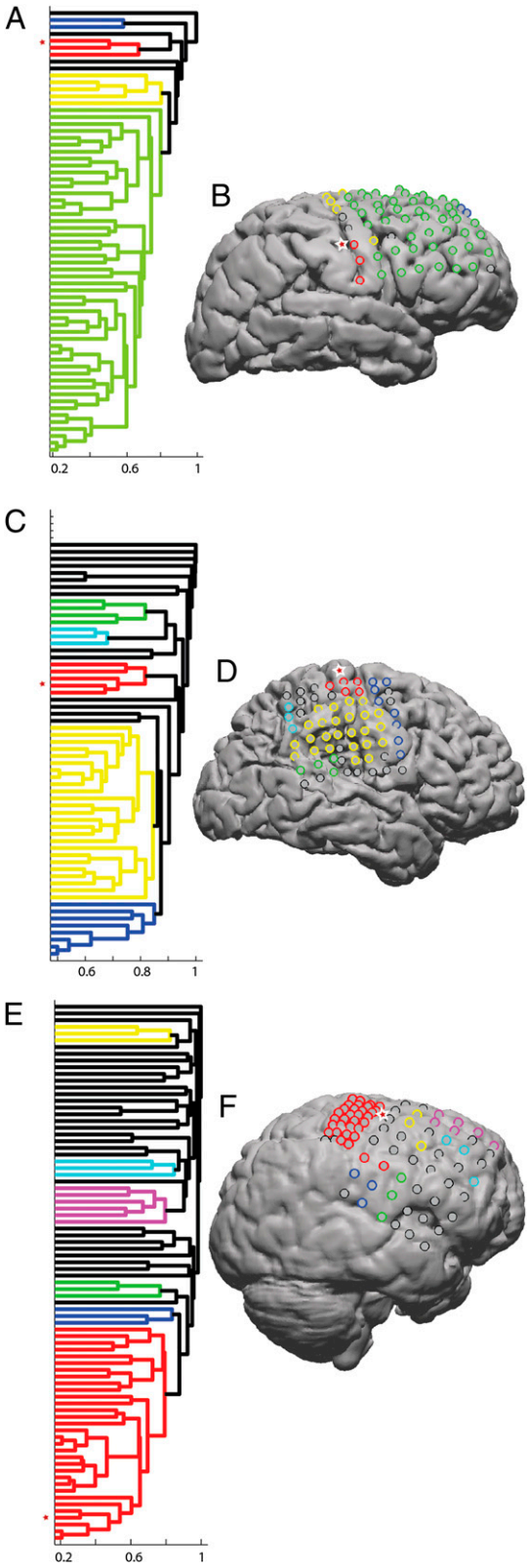

Fig. 4. Hierarchical clustering of spindle coincidence. A coincidence-based "distance" was used to cluster electrodes in spindle space. Dendrograms (*A*, *C*, and *E*) show the relative closeness of electrodes in this space. In this case, the dendrograms were created from posttraining sleep, but the coincidence between pre- and posttraining sleep was similar (Fig. 3 and Fig. S6). The distance between electrodes, plotted on the *x* axis, has a maximum value of 1 and a minimum value of 0. Clusters are formed by setting a distance threshold; here a threshold of 85% of the maximum distance was used. Example clusters are shown in different colors in the dendrograms and plotted with the same colors on the cortex (*B*, *D*, and *F*). For each subject, the task electrode is marked with a star on the left side of the dendrogram. For comparison, a similar star has been placed just to the left (*B*), on top (*D*), or to the right (*F*) of the task electrode on the corresponding cortical surface. Coincidence was dominated by locality, but may reflect functional connectivity as well. For example, in subject 3 (*E* and *F*) the red cluster includes both premotor and hand-motor electrodes. These electrodes are relatively distant in cortical space, but known to be functionally connected. Interestingly, both motor and premotor members of this group showed increases in spindle rate in response to training. In subject 1 (*A* and *B*) the four electrodes that showed increases in spindle rate following training were members of two noncoincident groups, only one of which was involved in the task. In subject 2, (*C* and *D*) all of the electrodes showing rate increases were part of the same coincidence group. These results suggest that preexisting spindle groups are differentially modulated in response to training. For side-by-side comparisons of the relative and absolute magnitude of the spindle-rate difference and the identified clusters, as well as enlarged, numbered dendrograms, see Figs. S1–S5.

Task. Subjects were trained to control a one-dimensional BCI using overt movements and motor imagery. A brief description of the task is given here, a detailed explanation can be found in refs. 25 and 36. During task performance the signal was split from the clinical system and passed to the BCI2000 software package (37), which was used for online signal processing and stimulus presentation. The control signal was derived from power changes in either the high-gamma (70–100 Hz) or beta (8–24 Hz) range over a single electrode (the task electrode). At the University of Washington, the task electrode was chosen based on a simple cue-based motor screening task in which the subject was asked to alternately move, or imagine moving, the tongue or the hand. The electrode with the most significant high-gamma band-power difference between activity and rest was selected. At Utrecht University Medical Center, the subject underwent a presurgical functional MRI (fMRI) in which a target was identified with a finger-tapping task. After electrode implantation, this target was confirmed with a functional screening task and clinical electrical stimulation. During each task trial, a cursor was presented vertically centered on the far left side of the screen and moved at a fixed rate across the screen to the right side. The vertical velocity of the cursor was updated every 40 ms based on the power in the specified frequency band recorded at the task electrode. The subject was asked to control the cursor such that when it reached the far right side of the screen its vertical position was within a designated target range. For two of the subjects, only two targets were used, the top and the bottom half of the screen. In one subject the number of targets was increased by dividing the vertical extent of the screen into smaller fractions. Thus, the size of each target was reduced and the subject was required to exert a greater degree of control over the cursor.

Sleep Spindle Detection. An automatic sleep spindle detection algorithm, similar to the method found in ref. 38, was used to count the number of discrete spindle events on each electrode. For each identified *NREM* sleep epoch, the down-sampled and normalized electrode traces were band-pass filtered between 11 and 16 Hz using a fourth order Butterworth filter. The Hilbert transform was used to find the envelope of the filtered signal, which was then squared to provide an estimate of instantaneous power in the spindle range. Discrete spindle events were detected using the following algorithm: First, the power signals were subjected to a threshold which was defined as five times the average power in all of the electrodes over the entire sleep epoch. A potential spindle was detected if the power surpassed this threshold for 0.25 s, consecutively. A window was then grown around each threshold crossing until the power dropped below a second threshold, which was similarly defined as two times the average power in all of the electrodes over the entire sleep epoch. Spindle events that were separated by less than 0.125 s were merged. If the detected spindle was shorter than 0.33 s or longer than 3.0 s, the spindle was rejected. Finally, the spectrum of the autocorrelation of each detected spindle was used to eliminate events that were not periodic by requiring that 50% of the power in the 5- to 30-Hz band was in the 11- to 16-Hz range. This is a conservative filter and intentionally biased toward type II error to avoid inclusion of paroxysmal events and artifacts.

Spindle Rate. Each sleep epoch was divided into 60-s nonoverlapping sections. If the duration of the epoch was not evenly divisible into 60 s, the end of the epoch was truncated. The number of spindle events occurring on each

electrode during each 60-s section was tallied to give the spindles per minute. The calculated spindle rates were pooled for all of the epochs occurring in each recording day, forming a distribution of spindle rates.

Statistical Testing. The number of events occurring in a time interval follows the Poisson distribution. Thus, we used the rate ratio (conditional) test (39) to determine for every electrode whether the mean rate of spindle occurrence was statistically different between sleep before BCI training and sleep after BCI training. The null hypothesis (that the rates were equal) was rejected for a P value less than 0.001, Bonferroni corrected to account for multiple comparisons.

The effect size is represented by the difference between the mean rates, scaled by the sum of the means. This measure of the magnitude ranges from zero to one and indicates how large the difference in the means is relative to the amplitude of the means.

$$E_{d_2 d_1} = \frac{\left(\overline{d_2} - \overline{d_1}\right)}{\left(\overline{d_2} + \overline{d_1}\right)}.$$

Coincidence Measure and Hierarchical Clustering. The spindle coincidence, $C_{i,j}$, between electrode i and electrode j was calculated as the number of spindles occurring within 0.5 s of each other on the two electrodes ($N_{i \cap j}$) divided by the total number of spindles on both electrodes ($N_i + N_j$):

$$C_{i,j} = \frac{N_{i \cap j}}{N_i + N_j}.$$

This quantity has a maximum value of 0.5 and a minimum value of 0, for display it is rescaled from 0 to 1. The time frame for coincidence (0.5 s) was chosen to be generous on the time scale of a spindle (0.33–3.0 s) and to allow for jitter in onset/offset times. Spindles are not required to be synchronous, only roughly coincident. Thus, this metric errs on the side of inclusion rather than exclusion. The similarity of the pretraining coincidence matrix and posttraining coincidence matrix was measured by the correlation. For a statistical treatment of similarity see Fig S6.

The coincidence was turned into a distance metric by calculating the quantity: $1 - C_{i,j}$. Using this distance, agglomerative hierarchical cluster trees were created using the "linkage" function in Matlab. Distance between clusters was measured using the unweighted average distance. Clusters, or coincidence groups, are created by imposing a distance threshold. Here, thresholds are set to 85% of the maximum distance; this translates to 85% of the range of coincidence where zero is completely coincident and 1 is completely noncoincident (i.e., no spindles are ever recorded on both electrodes at the same time). The threshold choice was made by empirical observation and was chosen for illustrative purposes. Choosing a lower threshold splits the clusters, choosing a higher threshold merges the clusters, but the threshold does not change the "coincidence distance" between electrodes. Cluster trees are represented with dendrograms. See Figs. S2–S6 for enlarged, numbered versions of the dendrograms.

Electrode Localization. Electrode locations were determined based on postoperative X-ray images. These images were coregistered with a preoperative structural MRI scan and electrode locations were projected onto a rendering of the cortical surface (40).

ACKNOWLEDGMENTS. This research was supported by National Institutes of Health Grant R01 NS065186-01 and award number EEC-1028725 from the National Science Foundation.

1. Stickgold R (2005) Sleep-dependent memory consolidation. *Nature* 437(7063): 1272–1278.
2. Steriade M (2003) The corticothalamic system in sleep. *Front Biosci* 8:d878–d899.
3. Mölle M, Marshall L, Gais S, Born J (2002) Grouping of spindle activity during slow oscillations in human non-rapid eye movement sleep. *J Neurosci* 22(24):10941–10947.
4. Coulon P, Budde T, Pape H-C (2012) The sleep relay—the role of the thalamus in central and decentral sleep regulation. *Pflugers Arch* 463(1):53–71.
5. Gais S, Mölle M, Helms K, Born J (2002) Learning-dependent increases in sleep spindle density. *J Neurosci* 22(15):6830–6834.
6. Clemens Z, Fabó D, Halász P (2005) Overnight verbal memory retention correlates with the number of sleep spindles. *Neuroscience* 132(2):529–535.
7. Eschenko O, Mölle M, Born J, Sara SJ (2006) Elevated sleep spindle density after learning or after retrieval in rats. *J Neurosci* 26(50):12914–12920.
8. Siapas AG, Wilson MA (1998) Coordinated interactions between hippocampal ripples and cortical spindles during slow-wave sleep. *Neuron* 21(5):1123–1128.
9. Sirota A, Csicsvari J, Buhl D, Buzsáki G (2003) Communication between neocortex and hippocampus during sleep in rodents. *Proc Natl Acad Sci USA* 100(4):2065–2069.
10. Johnson LA, Euston DR, Tatsuno M, McNaughton BL (2010) Stored-trace reactivation in rat prefrontal cortex is correlated with down-to-up state fluctuation density. *J Neurosci* 30(7):2650–2661.
11. Sejnowski TJ, Destexhe A (2000) Why do we sleep? *Brain Res* 886(1–2):208–223.
12. Steriade M, Timofeev I (2003) Neuronal plasticity in thalamocortical networks during sleep and waking oscillations. *Neuron* 37(4):563–576.
13. Peyrache A, Battaglia FP, Destexhe A (2011) Inhibition recruitment in prefrontal cortex during sleep spindles and gating of hippocampal inputs. *Proc Natl Acad Sci USA* 108(41):17207–17212.
14. Smith C, MacNeill C (1994) Impaired motor memory for a pursuit rotor task following Stage 2 sleep loss in college students. *J Sleep Res* 3:206–213.
15. Walker MP, Brakefield T, Morgan A, Hobson JA, Stickgold R (2002) Practice with sleep makes perfect: Sleep-dependent motor skill learning. *Neuron* 35(1):205–211.
16. Fogel SM, Smith CT (2006) Learning-dependent changes in sleep spindles and Stage 2 sleep. *J Sleep Res* 15(3):250–255.
17. Nishida M, Walker MP (2007) Daytime naps, motor memory consolidation and regionally specific sleep spindles. *PLoS ONE* 2(4):e341.
18. Dehghani N, Cash SS, Rossetti AO, Chen CC, Halgren E (2010) Magnetoencephalography demonstrates multiple asynchronous generators during human sleep spindles. *J Neurophysiol* 104(1):179–188.
19. Bonjean M, et al. (2012) Interactions between core and matrix thalamocortical projections in human sleep spindle synchronization. *J Neurosci* 32(15):5250–5263.
20. Nir Y, et al. (2011) Regional slow waves and spindles in human sleep. *Neuron* 70(1): 153–169.
21. Pfurtscheller G, Graimann B, Huggins JE, Levine SP, Schuh LA (2003) Spatiotemporal patterns of beta desynchronization and gamma synchronization in corticographic data during self-paced movement. *Clin Neurophysiol* 114(7):1226–1236.
22. Miller KJ, et al. (2007) Spectral changes in cortical surface potentials during motor movement. *J Neurosci* 27(9):2424–2432.
23. Wolpaw JR, McFarland DJ, Neat GW, Forneris CA (1991) An EEG-based brain-computer interface for cursor control. *Electroencephalogr Clin Neurophysiol* 78(3):252–259.
24. Leuthardt EC, Schalk G, Wolpaw JR, Ojemann JG, Moran DW (2004) A brain-computer interface using electrocorticographic signals in humans. *J Neural Eng* 1(2):63–71.
25. Blakely T, Miller KJ, Zanos SP, Rao RPN, Ojemann JG (2009) Robust, long-term control of an electrocorticographic brain-computer interface with fixed parameters. *Neurosurg Focus* 27(1):E13.
26. Talairach J, Tournoux P (1988) *Co-Planar Stereotaxic Atlas of the Human Brain. 3-Dimensional Proportional System: An Approach to Cerebral Imaging* (Thieme Medical, New York).
27. Crone NE, Miglioretti DL, Gordon B, Lesser RP (1998) Functional mapping of human sensorimotor cortex with electrocorticographic spectral analysis. II. Event-related synchronization in the gamma band. *Brain* 121(Pt 12):2301–2315.
28. Diekelmann S, Born J (2010) The memory function of sleep. *Nat Rev Neurosci* 11(2): 114–126.
29. Mölle M, Eschenko O, Gais S, Sara SJ, Born J (2009) The influence of learning on sleep slow oscillations and associated spindles and ripples in humans and rats. *Eur J Neurosci* 29(5):1071–1081.
30. Rosanova M, Ulrich D (2005) Pattern-specific associative long-term potentiation induced by a sleep spindle-related spike train. *J Neurosci* 25(41):9398–9405.
31. Méndez M, Radtke RA (2001) Interactions between sleep and epilepsy. *J Clin Neurophysiol* 18(2):106–127.
32. Fogel SM, Smith CT (2011) The function of the sleep spindle: A physiological index of intelligence and a mechanism for sleep-dependent memory consolidation. *Neurosci Biobehav Rev* 35(5):1154–1165.
33. Nicolas A, Petit D, Rompré S, Montplaisir J (2001) Sleep spindle characteristics in healthy subjects of different age groups. *Clin Neurophysiol* 112(3):521–527.
34. Ishizuka Y, et al. (1994) Sleep spindle frequency changes during the menstrual cycle. *J Sleep Res* 3(1):26–29.
35. Wennberg R (2010) Intracranial cortical localization of the human K-complex. *Clin Neurophysiol* 121(8):1176–1186.
36. Vansteensel MJ, et al. (2010) Brain-computer interfacing based on cognitive control. *Ann Neurol* 67(6):809–816.
37. Schalk G, McFarland DJ, Hinterberger T, Birbaumer N, Wolpaw JR (2004) BCI2000: A general-purpose brain-computer interface (BCI) system. *IEEE Trans Biomed Eng* 51(6): 1034–1043.
38. Ferrarelli F, et al. (2007) Reduced sleep spindle activity in schizophrenia patients. *Am J Psychiatry* 164(3):483–492.
39. Krishnamoorthy K, Thomson J (2004) A more powerful test for comparing two Poisson means. *J Statist Plann Inference* 119:23–35.
40. Hermes D, Miller KJ, Noordmans HJ, Vansteensel MJ, Ramsey NF (2010) Automated electrocorticographic electrode localization on individually rendered brain surfaces. *J Neurosci Methods* 185(2):293–298.